EXPERIMENTAL RESEARCH ABOUT ORTHOGONAL CUTTING PROCESS OF ALUMINIUM ALLOY 6060

Adrian TRIF[1], Claudiu Mihai NEDEZKI[1], Adriana RUS[1]

ABSTRACT: The article presents a complete analysis of the orthogonal cutting process of aluminium alloy 6060 analysis that is based on the mathematical model established by Merchant (model which relates to the formation of the continuous chip, flow chip, without built-up edge, who consider that the chip is made by a process of the shear which occurs in an thin area assimilated to a plane called shear plane). Special Walter inserts were used for cutting of commercial aluminum. The main and the rejection component of force (Fp and Fr) were measured using the dynamometer DKM2010 from the laboratory of BAGS. Excel was used for the calculation and graphical representation of the experimental data.
KEY WORDS: aluminium, chip, orthogonal, cutting process, force

1. THE PURPOSE OF PAPER

Aluminium alloy 6060 is a medium strength heat treatable alloy with a strength slightly lower than 6005A. It has very good corrosion resistance and very good weldability plus good cold formability especially in temper T4. It is commonly used alloy for very complex cross sections and has very good anodizing response [6].

The alloy composition of 6060 aluminium is [6], [7]:

- Aluminium: 97.9 to 99.3%
- Chromium: 0.05% max
- Copper: 0.1% max
- Iron: 0.1 to 0.3%
- Magnesium: 0.35 to 0.6%
- Manganese: 0.10%
- Silicon: 0.3 to 0.6%
- Titanium: 0.1% max
- Zinc: 0.15% max
- Residuals: 0.15% max

The paper highlights the following aspects about the orthogonal cutting process of Aluminium alloy 6060:

• the thickness a_1 and b_1 the width of the layer of material to be removed by the tool are constant;

• the cutting motion is achieved with a constant cutting speed *(v)*.

• establishing the influence of cutting parameters and of geometry on the chip deformation and determining the effectiveness of the cutting process according to these parameters;

• observation of chip formation process as a process of plastic deformation;

• calculation of the forces that appear in the cutting process by the main component F_P and by the rejection component F_r measured by dynamometer;

• calculating shear stresses (τ) and compression stresses (σ) occurring during cutting;

• determining the direction of deformation characterized by ψ angle

• determining the shear direction, situated at the shear angle ϕ relative to the plane of the cutting edge;

2.THEORETICAL CONSIDERATIONS ON ORTHOGONAL CUTTING PROCESS

The orthogonal cutting (figure 1) is the simple cutting process, usually of a flat surface that fulfills the following conditions [2], [3]:

• the cutting edge of the cutting tool is normal to the direction of relative motion between tool and workpiece, called cutting motion;

• cutting edge length is greater than or at least equal to the width of workpiece b_1;

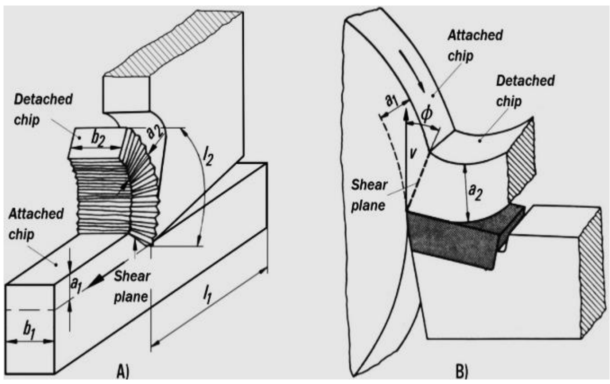

Fig.1 Orthogonal cutting:
A) planing of plane surface; B) transverse turning of a disk;

[1] Technical University of Cluj-Napoca, Bd. Muncii, 103-105, Cluj-Napoca, Romania
E-mail: adrian.trif@tcm.utcluj.ro;
claudiu.nedezki@muri.utcluj.ro; adi_adrianarus@yahoo.com

Chip formation mechanism (figure 2) can be represented as a process of successive movements Δs of thin layers of material, having a thickness Δx, along the shear plane respecting the integrity of the neighboring layer [2].

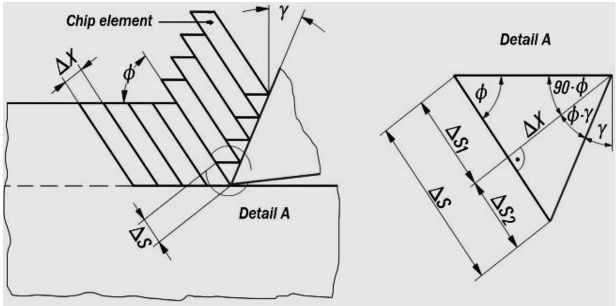

Fig.2 Merchant model of chip formation

When the specific shear deformation $\varepsilon = {\Delta s}/{\Delta x}$ reaches a certain characteristic value of each cutting process,occurs the shear of the material in the shear plane.

$$\varepsilon = \frac{\Delta s}{\Delta x} = \frac{\Delta s_1 + \Delta s_2}{\Delta x}; \quad \Leftrightarrow$$
$$\varepsilon = \frac{\Delta x \cdot \mathrm{ctg}\phi + \Delta x \cdot \mathrm{tg}(\phi - \gamma)}{\Delta x}; \qquad (1)$$
$$\varepsilon = \mathrm{ctg}\phi + \mathrm{tg}(\phi - \gamma)$$

The microscopic analysis of the chip's base (Figure 3) shows that the crystals of the metal (the workpiece) have an well defined orientation (depending on the type of metal), and when arrives in the shear plane suffers a plastic deformation (and cold straining), deformation that leads to a new orientation of their.

The new direction of the crystals orientation make an angle ψ with the shear plane. The angle of deformation (ψ) depends on the cutting conditions and on the type of chipped material [3].

Specific shear deformation between ε, ϕ angle shear, deflection angle and departure angle ψ γ, there is the relationship:

$$\varepsilon = \mathrm{ctg}\psi = \mathrm{ctg}\phi + \mathrm{tg}(\phi - \gamma) \qquad (2)$$

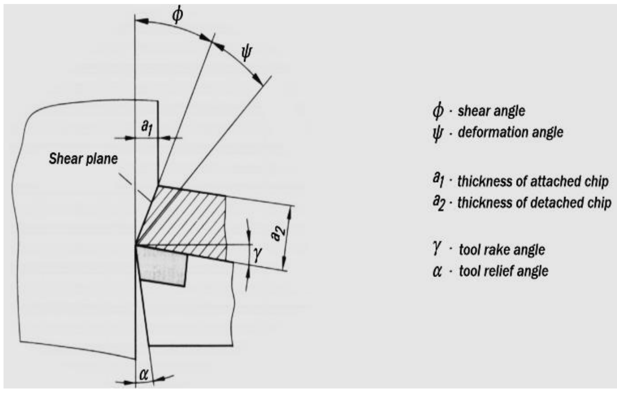

Fig.3 New orientation direction of the workpiece's crystals in the detached chip

Due to plastic deformations occurred during the chip's formation, the detached chip (having the thickness a_2; width b_2; length l_2) differs by shape and dimensions compared to the layer of material to be removed in the chip form – attached chip (having the thickness a_1; width b_1 ; length l_1). Changing the size of chip is estimated using the following factors:

$k_a = a_2/a_1$ - coefficient of thickening of the chip;

$k_b = b_2/b_1$ - coefficient of widening of the chip;

$k_l = l_1/l_2$ - coefficient compression of the chip.

Due to the assumptions used in the study of orthogonal cutting and experimental observation that the chip is not widened, $k_b = 1 \Rightarrow k_a = k_l$.

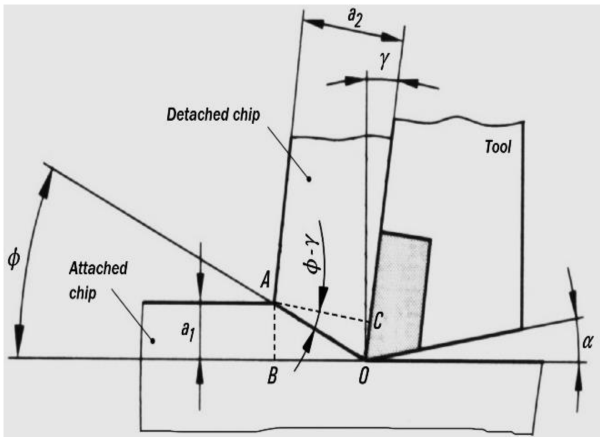

Fig.4 Geometrical necessary elements for determination of the shear angle ϕ

Determining experimentally (by measurement) of k_a , based on geometric elements shown in figure 4, the angle ϕ is analytically determined:

$$k_a = \frac{a_2}{a_1} = \frac{AC}{AB} = \frac{AO \cdot \cos(\phi - \gamma)}{AO \cdot \sin\phi} =$$

$$\frac{\cos(\phi-\gamma)}{\sin\phi} = \frac{\cos\phi \cdot \cos\gamma + \sin\phi \cdot \sin\gamma}{\sin\phi}; \quad (3)$$

$$\mathrm{tg}\phi = \frac{\cos\gamma}{k_a - \sin\gamma} \quad (4)$$

k_a = f (tool geometry: γ, α; a_1; v; cutting environment; workpiece material.)The analysis of the forces acting on the orthogonal cutting process (figure 5) is made using the following hypothesis:

• the chip is a separate body, in balance on the rake face (A_γ) under the action of two equal, collinear and opposite forces $\boldsymbol{F_R}$ and $\boldsymbol{F_R}'$.
• $\boldsymbol{F_R}'$ is the action of cutting tool on the workpiece, $\boldsymbol{F_R}$ is the reaction of the workpiece.

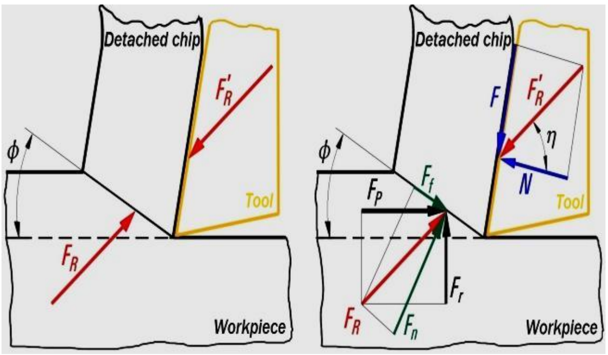

Fig.5 The forces in orthogonal cutting process

To highlight the forces that produce the specific stresses for the formation of the chip (the shear and friction) are available following decompositions:

• $\boldsymbol{F_R}$ force is decomposed into a component acting in the shear plane and a component $\boldsymbol{F_f}$ normal on the shear plane $\boldsymbol{F_n}$ (component that will exert a compressive stress on it);
• The force $\boldsymbol{F_R}'$ is decomposed into component **F** representing the friction force that opposes to the flow of chip and the component **N** normal on the rake face;
• $\boldsymbol{F_R}$ force is decomposed into a main component $\boldsymbol{F_P}$ (in the cutting direction) and a passive component (rejection component) $\boldsymbol{F_r}$ (normal to the cutting direction).
• In practice can only measure the components $\boldsymbol{F_P}$ and $\boldsymbol{F_r}$.
• With equal forces $\boldsymbol{F_R}$ and $\boldsymbol{F_R}'$, and the small size of the zone of deformation, the components can be represented as a components of a single vector $\boldsymbol{F_R}$, conventionally having the application point to the top of cutting edge; → **Merchant's circle** (figure 6);

The components $\boldsymbol{F_P}$ components and $\boldsymbol{F_r}$ is measured using the dynamometer and the other is determined by the formulas (5) – (11):

To establish the power consumption in the cutting process shall be taken away into account the mechanical work consumed per unit volume of removed material, called specific mechanical work.

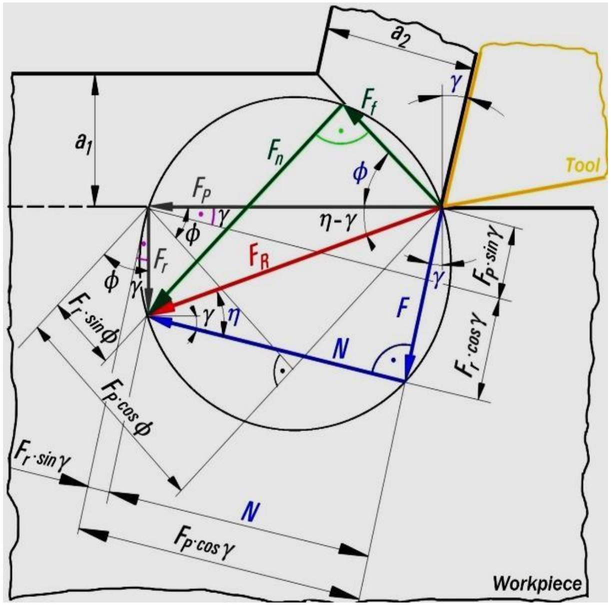

Fig.6 The diagram of orthogonal cutting forces (Merchant's circle)

Total specific mechanical work ($\boldsymbol{L_\Sigma}$) is consumed to achieve the deformation in the shear plan and for the defeat of friction between chip and tool.

The specific shear mechanical work $\boldsymbol{L_f}$ is determined by the relation (12):

The specific mechanical work for the defeat of friction is calculated using equation (13):

$$\begin{cases} F = F_P \sin\gamma + F_r \cos\gamma & (5) \\ N = F_P \cos\gamma - F_r \sin\gamma & (6) \end{cases} \Rightarrow$$

$$\mu = \mathrm{tg}\eta = \frac{F}{N} = \frac{F_P \mathrm{tg}\gamma + F_r}{F_P - F_r \mathrm{tg}\gamma} \quad (7)$$

$$\begin{cases} F_f = F_P \cos\phi - F_r \sin\phi & (8) \\ F_n = F_f \,\mathrm{tg}(\phi + \eta - \gamma) & (9) \\ A_f = \dfrac{a_1}{\sin\phi} b \end{cases} \Rightarrow$$

$$\begin{cases} \tau = \dfrac{F_f}{A_f} = \dfrac{(F_P \cos\phi - F_r \sin\phi)\sin\phi}{a_1 b} & (10) \\ \sigma = \dfrac{F_n}{A_f} = \tau \cdot \mathrm{tg}(\phi + \eta - \gamma) & (11) \end{cases}$$

$$L_f = \frac{F_f \cdot \Delta s}{A_1 \cdot l_1} = \frac{F_f \cdot \Delta s}{A_1 \cdot \dfrac{\Delta x}{\sin\phi}} = \frac{F_f}{A_f} \cdot \varepsilon = \tau \cdot \varepsilon \qquad (12)$$

Total specific mechanical work (L_Σ) is calculated using equation (14):

$$L_\Sigma = \tau \cdot \varepsilon + \frac{F}{A_2} \qquad (14)$$

3. THE IMPLEMENTATION OF THE EXPERIMENT

For highlighting the plastic deformation occurring in the cutting area and calculation of efficiency of the process by setting total specific mechanical work, will determine the coefficient of thickening of the chip for different cutting situations. The size of detached chip determination is made by measurement with the followin instruments:

- Oditest (Kroeplin);
- Workshop microscope (Carl Zeiss type).

The orthogonal cutting process will be studied in five series of experiments (three tests each experiment), long turning a test piece in the form of pipe with an external diameter of 44 mm and walls of constant thickness.

The first series of experiments are performed with a tool having the rake angle $\gamma = 0^0$ and longitudinal feed of 0.1 mm / rev (The feed rate is the value of thickness of undetached chip) using 3 different rotational speeds of the workpiece.

The second and third series of experiments are performed with a tool having the rake angle $\gamma = 7^0$; $\gamma = 22^0$ respectively, while maintaining constant the same feed rate and the same rotational speed of the workpiece, as in the first series of experiments.

The fourth and fifth series of experiments are performed with a tool having the longitudinal feed 0,16; 0,2; respectively 0,315 mm / rev, and the rake angle $\gamma = 22^0$ while maintaining constant the rotational speed of the workpiece (800 rev / min respectively 630 rev / min).

For each test is measured, using the dynamometer, the main component $\boldsymbol{F_P}$ and the rejecting component $\boldsymbol{F_r}$ and using Oditest's is measured the thickness of the detached chip $\boldsymbol{a_2}$.

The results shall be mentioned in a centralizing table and the dependencies will be graphically represent:

- k_a = f (v) - tests: [(1,2,3) for $\gamma = 0^0$; (4,5,6) for $\gamma = 7^0$; (7,8,9) for $\gamma = 22^0$];
- k_a = f (a_1) - tests [(10,11,12) for n = 800 rev / min; (13,14,15) for n = 630 rev / min];
- k_a = f (γ) - tests: [(1,4,7) for n = 500 rev / min; (2,5,8) for n = 630 rev / min; respectively (3,6,9 for n = 800 rev / min];
- P_F = f (v); F_P = f (a_1); F_P = f (γ);
- ϕ = f (v); ϕ = f (a_1); ϕ = f (γ);
- ε = f (v); ε = f (a_1); ε = f (γ).

4. EXPERIMENTAL CONDITIONS

Machine: universal lathe SNA560

Tool: 3 inserts for aluminum turning: $\chi_r = 90^0$; $\gamma = 0^0$ (CCMW 09 03 04 K15); $\gamma = 7^0$ (CCMT 09 T3 04 K15); $\gamma = 22^0$ respectively (CCGT 09 T3 08 – DL K10 K20).

Cutting fluid: dry turning

Workpiece: Al6060 pipe D_{ext} = 44 mm; The wall thickness of the pipe: b = 2 mm .

Dynamometer with resistive transducer: tensometric stamps connected in Wheatstone bridge (DKM2010)

Table1: Summary of experimental data

No.	γ [^{0}]	n [rot/min]	v [m/min]	a_1 [mm]	a_2 [mm]	k_a []	$\tan\phi$ []	ϕ [^{0}]	ε []	F_p [daN]	F_r [daN]	F [daN]	N [daN]	μ	F_f [daN]	F_n [daN]	τ [daN/mm^2]	σ [daN/mm^2]	L_f [daN/mm^2]	L_{ft} [daN/mm^2]	L_Σ [daN/mm^2]
1	0	500	69,08	0,1	0,71	7,1	0,141	8,026	83,039	40	55,8	55,8	40	0,14	31,85	9,14	22,13	6,352	1837,7	39,3	1877
2	0	630	87,04	0,1	0,63	6,3	0,159	9,034	83,843	38,3	50,2	50,2	38,3	0,131	29,96	8,87	23,52	6,96	1971,99	39,85	2011,84
3	0	800	110,53	0,1	0,6	6	0,167	9,481	84,146	34	44,1	44,1	34	0,13	26,25	7,98	21,66	6,6	1822,603	36,75	1859,353
4	7	500	69,08	0,1	0,36	3,6	0,285	15,907	86,56	34,8	38,1	42,08	29,91	0,141	23,04	7,03	31,56	9,63	2731,834	58,45	2790,284
5	7	630	87,04	0,1	0,35	3,5	0,294	16,383	86,672	31,8	35,8	39,43	27,21	0,145	20,43	6,54	28,82	9,23	2497,9	56,33	2554,23
6	7	800	110,53	0,1	0,33	3,3	0,312	17,328	86,879	28,4	31,7	34,943	24,334	0,144	17,68	5,904	26,34	8,8	2288,4	52,944	2341,344
7	22	500	69,08	0,1	0,46	4,6	0,219	12,353	85,202	33,1	30	40,223	19,434	0,207	25,92	0,933	27,72	1	2361,8	43,72	2405,52
8	22	630	87,04	0,1	0,4	4	0,256	14,359	85,882	22,1	19,6	26,46	13,14	0,201	16,56	1,08	20,54	1,34	1764,02	33,1	1797,12
9	22	800	110,53	0,1	0,35	3,5	0,297	16,542	86,444	20	15,5	21,87	12,73	0,172	14,76	1,112	21,03	1,59	1817,92	31,243	1849,163
10	22	800	110,53	0,16	0,73	4,57	0,221	12,462	85,048	29,8	25,1	34,443	18,212	0,19	23,7	0,522	15,99	0,353	1359,92	23,55	1383,47
11	22	800	110,53	0,2	0,67	3,35	0,312	17,328	86,618	43	39	52,3	24,24	0,216	29,44	3,63	21,32	2,63	1846,7	39,03	1885,73
12	22	800	110,53	0,315	0,51	1,62	0,745	36,686	88,702	81,1	88	111,99	42,18	0,266	12,24	6,98	11,66	6,65	1034,266	109,73	1143,996
13	22	630	87,04	0,16	0,78	4,88	0,206	11,64	84,907	30,8	25,4	35,1	19,03	0,185	25,05	0,053	15,82	0,034	1343,23	22,5	1365,73
14	22	630	87,04	0,2	0,71	3,55	0,292	16,278	86,385	55	60	76,25	28,49	0,27	36	5,955	25,28	4,182	2183,813	53,7	2237,513
15	22	630	87,04	0,315	0,65	2,07	0,547	28,679	88,123	87,2	98,2	123,732	44,01	0,281	29,6	12,2	22,55	9,3	1987,174	72,74	2059,914


a

a


b

Fig. 7 a,b. The used inserts

b

c

d

e

Fig.8 a,b,c,d,e. The types of chips obtained from each experiment

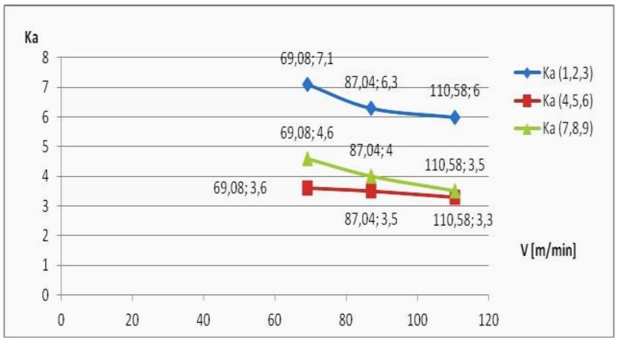

Fig. 9 The influence of cutting speed *v* on chip compression

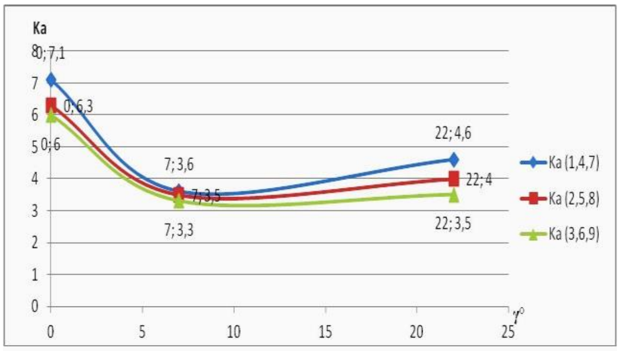

Fig.10 The influence of rake angle γ °on chip compression

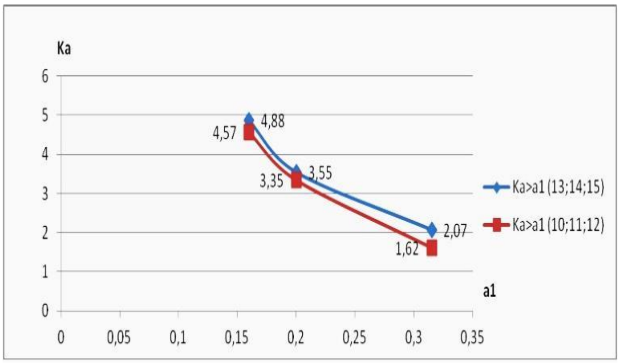

Fig.11 The influence of the attached chip's thickness $a_{1[mm]}$ on chip compression

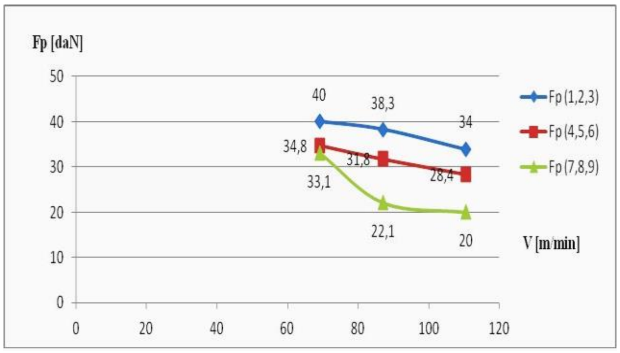

Fig.12 The influence of cutting speed *v* on the main cutting force (component)

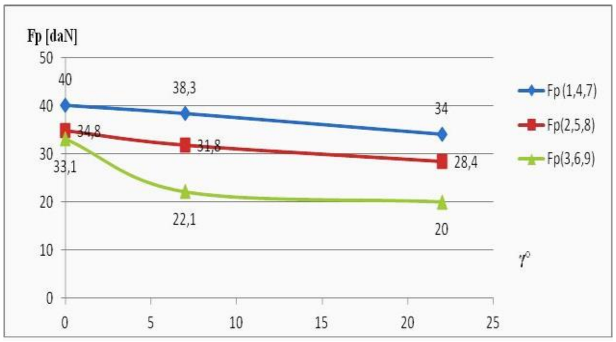

Fig.13 The influence of rake angle γ° on the main cutting force (component)

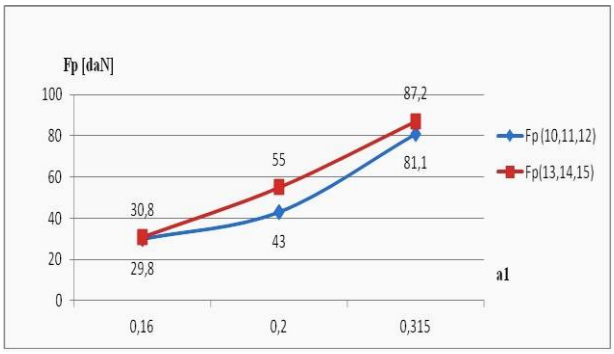

Fig.14 The influence of the attached chip's thickness $a_{1[mm]}$ (feed) on the main cutting force

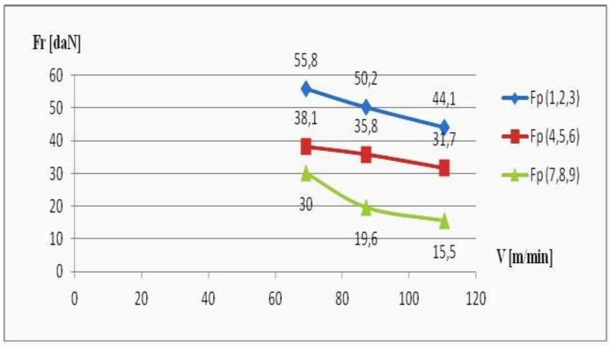

Fig.15 The influence of cutting speed v on the reaction force

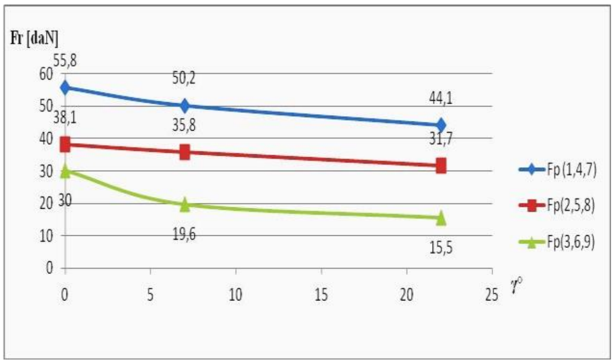

Fig.16 The influence of the rake angle γ° on the reaction force

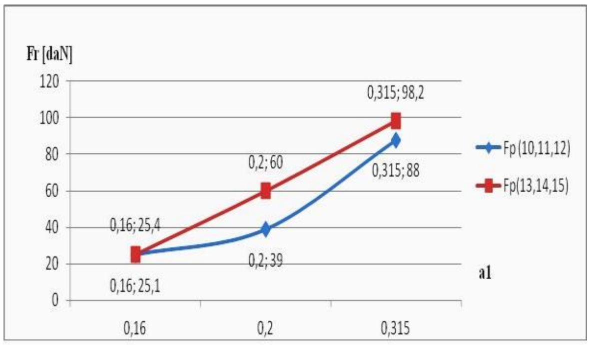

Fig.17 The influence of the attached chip's thickness $a_{1[mm]}$ (feed) on the reaction force

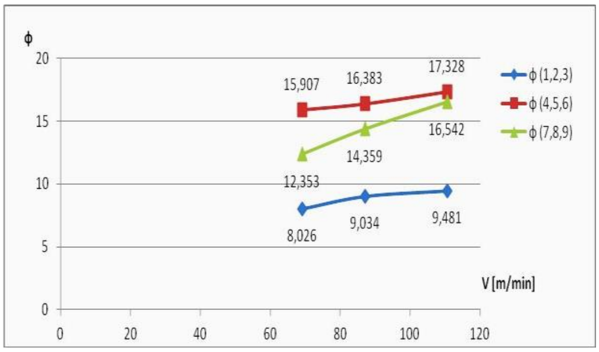

Fig.18 The influence of cutting speed v on the shear angle ϕ

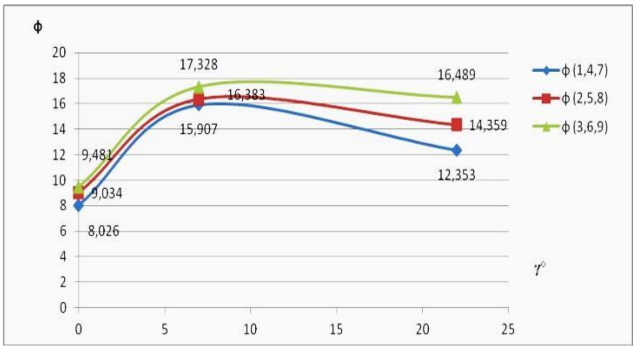

Fig.19 The influence of the rake angle γ° on the shear angle ϕ

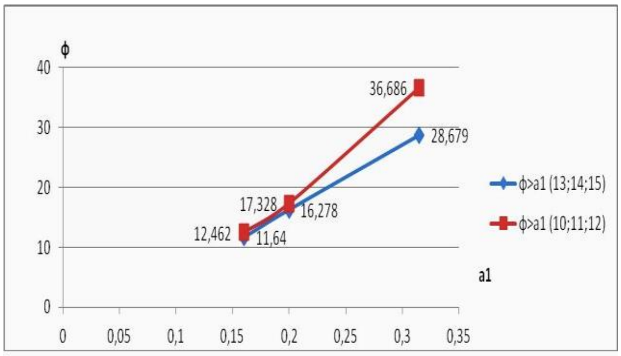

Fig.20 The influence of the attached chip's thickness $a_{1[mm]}$ on the shear angle ϕ

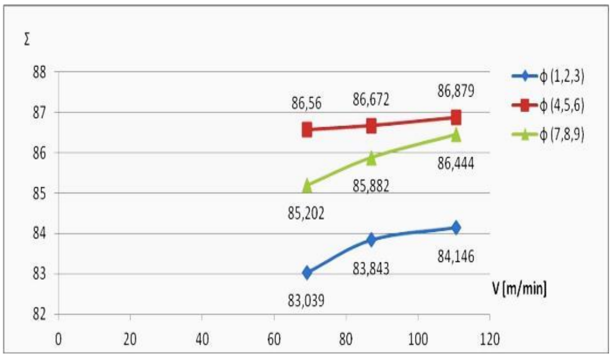

Fig.21 The influence of cutting speed v on the specific shear deformation ε

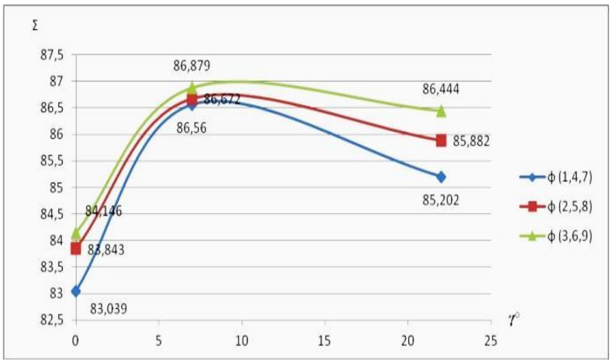

Fig.22 The influence of the rake angle γ°on the specific shear deformation ε

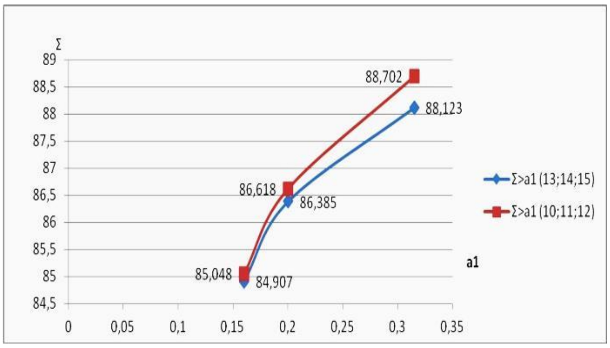

Fig.23 The influence of the attached chip's thickness $a_{1[mm]}$ on the specific shear deformation ε

5. CONCLUSIONS

• The orthogonal cutting process of aluminium alloy 6060 is a process without built-up edge, obtaining continuous chips, which justifies the use of mathematical model Merchant.

• The paper highlights how geometrical parameters of the tool cutting edge (rake angle γ, cutting speed and the thickness of undetached chip influence the compaction of chip, the cutting forces, the specific deformation or the shear angle

• It is found experimentally that with increasing of the rake angle γ it will reduce deformation and consequently the coefficient k_a, respectively the forces in the process

• To the processing of aluminium alloy 6060 the coefficient of thickening of the chip k_a and cutting forces decrease with increasing speed, faster at the beginning and then slower, due to changing conditions of friction between chip and rake face;

• To the processing of the same cutting speed, in the absence of built-up edge, with increasing thickness of the undetached chip a_1 there was a decrease of the deformations and thus the coefficient k_a, and the cutting forces increase (F_P and F_r)

• From the presented graphs is it notes that with the intensification of chip compaction, the shear angle φ decreases, which corresponds to the increase of strains during the chip formation process.

6. REFERENCES

[1] Kumar Jha, Sujit, Balakumar, Devibala and Paluchamy, Rajalingam**,** *Experimental Analysis of Mechanical Properties on AA 6060 and 6061 Aluminum Alloys*, S Kumar Jha et al. Int. Journal of Engineering Research and Applications www.ijera.com ISSN : 2248-9622, Vol. 5, Issue 4, (Part -7) April 2015, pp.47-53

[2] Merchant, Ernst H, ME (1941), *Chip formation, friction and high quality machined surfaces*, Surface treatment of metals. Am Soc Met 29:299–378

[3] Merchant ME (1945) *Mechanics of the metal cutting process II*, Plasticity conditions in orthogonal cutting. J. Appl. Phys.16(6):318–324

[4] Sethi, N, Senapati, A., *Investigation & Analysis of Different Aluminium Alloys*, International Journal of Engineering Research and Science & Technology, Jan, 2014, p. 106-112

[5] Tekkaya, A.E., a.o., *Hot profile extrusion of AA-6060 aluminum chips*, Journal of Materials Processing Technology, 04/2009

[6] Information on http://www.aalco.co.uk/datasheets/Aluminium-Alloy-6060-T5--Extrusions_144.ashx

[7] Information on https://en.wikipedia.org/wiki/6060_aluminium_alloy